Polymer Chemistry

PAPER

View Article Online
View Journal | View Issue

Cite this: *Polym. Chem.*, 2015, **6**, 5225

High-efficiency fluorescent polyimides based on locally excited triarylamine-containing dianhydride moieties†

Jia-Hao Wu and Guey-Sheng Liou*

Received 9th June 2015,
Accepted 18th June 2015

DOI: 10.1039/c5py00883b

www.rsc.org/polymers

Three novel high fluorescent polyimides (PIs) were readily synthesized from the polycondensation of triarylamine-based tetracarboxylic dianhydride monomers with a commercially available aliphatic diamine monomer. The photoluminescence (PL) intensity of the solid film and the nanofiber fabricated by solution casting and electrospinning methods revealed high quantum yields of up to 32% and 35%, respectively. Furthermore, in order to investigate the fluorescent transition mechanisms of the PIs, a series of model compounds corresponding to the repeat units of PIs were also synthesized, and density functional theory calculation results were also used to support the deduction. Moreover, the competition of aggregation enhanced emission (AEE) and aggregation caused quenching (ACQ) effects was investigated and demonstrated.

Introduction

Polymeric fluorescent materials have drawn significant attention due to the advantages including structural flexibility, low-cost, and feasibility of large area fabrication by solution spin-coating or inkjet printing[1] for their potential applications such as in light emitting diodes,[2] plastic lasers,[3] fluorescent sensors,[4] and optical wavelength converters.[5] However, the emerged π-conjugated fluorescent polymers, such as polyfluorene[6] derivatives, do not have sufficient thermal stability and glass transition temperatures to sustain high temperature treatment during device fabrication processes. Thus, the molecular design and synthesis of heat-resistant high-performance polymers with high fluorescence intensity in the solid state is beneficial and also crucial for advanced optoelectronic applications.

Polyimides (PIs), such as Kapton and Upilex, are well-known high-performance polymers with excellent combination of thermal and chemical stability, radiation resistance, and superior mechanical properties due to their rigid molecular structures and strong intermolecular interactions.[7] However, most of the aromatic PIs revealed too low photoluminescence quantum yield (PLQY) to be used as fluorescent materials. The optical absorption and emission behavior of PIs have been widely investigated by using molecular orbital (MO) transitions.[8] The most critical issue is charge transfer (CT) transition between electron-donating diamine and electron-accepting dianhydride moieties of PIs after UV-Vis irradiation, resulting in red-shifted and suppressed PL intensity. The other one is locally excited (LE) transition that occurs between occupied and unoccupied MOs, and both orbitals are located around the dianhydride moieties of PIs, thus could induce high PL intensity. Based on the above findings, PL efficiency of PIs could be effectively improved by introducing alicyclic diamines or dianhydrides into the PIs to reduce CT interactions and enhance LE transitions.[8a,9] Furthermore, most of the luminogens in the solid state generally lead to partial or even complete quenching of light emissions and reveal much lower PLQY than in solutions called aggregation-caused quenching (ACQ) effect. Recently, a novel phenomenon of aggregation-induced emission (AIE) or aggregation-enhanced emission (AEE)[10] which is exactly opposite to the ACQ effect paves a new strategy for designing and synthesis of highly efficient luminogens in the aggregated state and are attributed to the restriction of intramolecular rotation in the condensed phase and almost non-fluorescent in solution.

Triphenylamine (TPA) derivatives are well-known for their electrical and photophysical properties in many potential areas, such as hole-transporters, light-emitters, electrochromic and memory devices.[11] Recently, we developed and reported TPA-based fluorescent polyimides by the excellent combination of LE transition and AIE effect,[12] and the demonstrated

Functional Polymeric Materials Laboratory, Institute of Polymer Science and Engineering, National Taiwan University, 1 Roosevelt Road, 4th Sec., Taipei 10617, Taiwan. E-mail: gsliou@ntu.edu.tw; Fax: +886-2-33665237; Tel: +886-2-33665315

† Electronic supplementary information (ESI) available: Table: inherent viscosity, molecular weights, solubility behavior, thermal, and optical properties. Figure: NMR, FT-IR, TGA, TMA, absorption spectra, photoluminescence spectra. See DOI: 10.1039/c5py00883b

AIE effect of TPA derivatives could be attributed to their propeller-like structure similar to other AIE-active luminogens.[13]

In order to gain more insight into the working principle of AIE-active fluorescent PIs, a series of fluorescent PIs were prepared from triarylamine-based dianhydride monomers and aliphatic diamine monomer bis(4-aminocyclohexyl)methane in this study. In addition, a series of model compounds corresponding to the repeat units of PIs were also synthesized. The UV-Vis absorption and PL spectra, MO transitions with density functional theory calculations, and PL solvatochromism of these triarylamine-containing phthalimide model compounds were extensively investigated. Furthermore, the competition of AIE and ACQ effects in the PI system was also described.

Experimental section

Materials

Triarylamine-based dianhydride monomers, *N*,*N*-bis(3,4-dicarboxyphenyl)aniline dianhydride (**1**), *N*,*N*-bis(3,4-dicarboxyphenyl)-1-aminonaphthalene dianhydride (**2**), *N*,*N*-bis(3,4-dicarboxyphenyl)-1-aminopyrene dianhydride (**3**), and diamine monomer, 4,4′-diamino-triphenylamine (**1′**) were prepared according to the previously reported procedures.[12c] Commercially available bis(4-aminocyclohexyl)methane was purified by recrystallization from hexane. All other reagents were used as received from commercial sources.

Synthesis of model compounds

M-Ph was chosen as an example to illustrate the general synthetic route used to produce the model compounds. A 50 mL round-bottom flask equipped with a magnetic stirrer was charged with 0.303 g (0.79 mmol) of dianhydride (**1**), 0.160 g (1.61 mmol) of cyclohexylamine, and 2.5 mL of acetic acid. The reaction mixture was heated with stirring at 140 °C for 6 h. The resulting reaction solution was poured into 30 mL of stirring methanol/water giving rise to a yellow precipitate that was collected by filtration and dried.

M-Ph. Yield = 96%; mp = 214–216 °C (by the melting point system at a scan rate of 5 °C min^{-1}). ^{1}H NMR (400 MHz, $CDCl_3$, δ, ppm): 7.65–7.64 (d, 2H), 7.41–7.40 (s, 2H), 7.38–7.35 (t, 2H), 7.28–7.26 (d, 2H), 7.25–7.22 (t, 1H), 7.11–7.09 (d, 2H), 4.08–4.01 (m, 2H), 2.19–1.19 (m, 22H). ^{13}C NMR (100 MHz, $CDCl_3$, δ, ppm): 167.72, 167.67, 151.96, 145.23, 134.25, 130.37, 127.03, 126.55, 126.46, 125.65, 124.49, 117.06, 50.86, 29.75, 25.91, 25.00. FTIR (KBr): 2927–2850 cm^{-1} (cyclohexyl C–H stretch), 1764 (*asym.* imide C═O stretch), and 1701 cm^{-1} (*sym.* imide C═O stretch). Elemental Analysis (%) Calcd for $C_{34}H_{33}N_3O_4$: C, 74.57%; H, 6.07%; N, 7.67%. Found: C, 74.33%; H, 6.10%; N, 7.43%.

M-Np

Yield = 98%; mp = 175–185 °C. ^{1}H NMR (400 MHz, $CDCl_3$, δ, ppm): 8.07–8.04 (t, 2H), 7.81–7.80 (d, 1H), 7.68–7.67 (d, 2H), 7.65–7.62 (t, 1H), 7.58–7.55 (t, 2H), 7.50–7.47 (t, 1H), 4.08–4.01 (m, 2H), 7.30 (d, 2H), 7.28–7.26 (d, 2H) 3.90–3.84 (m, 2H), 2.01–1.08 (m, 22H). ^{13}C NMR (100 MHz, $CDCl_3$, δ, ppm): 167.71, 167.55, 152.14, 140.75, 135.47, 134.08, 130.42, 129.42, 129.30, 128.70, 128.27, 127.40, 127.32, 126.22, 125.26, 125.04, 123.05, 115.18, 50.54, 29.84, 25.91, 25.33. FTIR (KBr): 2929–2857 cm^{-1} (cyclohexyl C–H stretch), 1765 (*asym.* imide C═O stretch), and 1706 cm^{-1} (*sym.* imide C═O stretch). Elemental Analysis (%) Calcd for $C_{38}H_{35}N_3O_4$: C, 76.36%; H, 5.90%; N, 7.03%. Found: C, 75.99%; H, 5.94%; N, 6.83%.

M-Py. Yield = 98%; mp = 263–265 °C. ^{1}H NMR (400 MHz, $CDCl_3$, δ, ppm): 8.25–8.22 (m, 2H), 8.17–8.14 (t, 2H), 8.10–8.09 (d, 1H), 8.05–8.01 (t, 1H), 8.01–8.00 (d, 1H), 7.94–7.92 (d, 1H), 7.81–7.79 (4,1H), 7.63–7.61 (d, 2H), 7.48–7.47 (d, 2H), 7.28–7.26 (d, 2H), 4.07–4.00 (m, 2H), 2.18–1.19 (m, 22H). ^{13}C NMR (100 MHz, $CDCl_3$, δ, ppm): 167.84, 167.76, 152.44, 137.48, 134.40, 131.18, 131.07, 130.74, 129.52, 128.43, 128.13, 127.20, 126.99, 126.71, 126.40, 126.36, 126.19, 125.89, 125.82, 125.36, 124.68, 124.54, 121.50, 115.75, 50.90, 29.80, 25.97, 25.04. FTIR (KBr): 2928–2855 cm^{-1} (cyclohexyl C–H stretch), 1763 (*asym.* imide C═O stretch), and 1705 cm^{-1} (*sym.* imide C═O stretch). Elemental Analysis (%) Calcd for $C_{44}H_{37}N_3O_4$: C, 78.67%; H, 5.55%; N, 6.26%. Found: C, 78.11%; H, 5.45%; N, 6.11%.

M-Ph′. Yield = 90%; mp = 104–109 °C. ^{1}H NMR (400 MHz, DMSO-D6, δ, ppm): 7.38–7.35 (t, 2H), 7.22–7.20 (d, 4H), 7.14–7.09 (m, 7H), 3.10 (s, 4H), 1.80–1.73 (m, 8H), 1.50–1.32 (m, 8H). ^{13}C NMR (100 MHz, $CDCl_3$, δ, ppm): 117.52, 145.91, 145.59, 128.28, 125.84, 125.18, 124.15, 122.82, 122.54, 38.77, 22.71, 20.56. FTIR (KBr): 2936–2856 cm^{-1} (cyclohexyl C–H stretch), 1780 (*asym.* imide C═O stretch), and 1712 cm^{-1} (*sym.* imide C═O stretch).

Synthesis of polyimides by the one-step method

The synthesis of **Ph-DCHPI** was used as an example to illustrate the general synthetic route used to produce the PIs. Into a 50 mL round-bottom flask were added 0.3850 g (1.00 mmol) of dianhydride (**1**), 0.210 g (1.00 mmol) of bis(4-aminocyclohexyl)methane, 0.24 ml isoquinoline, and 2.4 ml *m*-cresol. The reaction mixture was stirred at 50 °C under a nitrogen atmosphere for 18 h. Then, the reaction temperature was increased to 200 °C for 15 h. Then, the mixture was cooled to room temperature, and the viscous polymer solution was then poured slowly into 300 ml of stirred methanol giving rise to a yellow fibrous precipitate. Reprecipitation of the polymer by DMAc/methanol was carried out twice for further purification.

Fabrication of electrospun fibers

A polymer solution with the concentration of 25 wt% in $CHCl_3$ was used to produce the electrospun (ES) fiber. The ES fiber was prepared using a single-capillary spinneret. First, the solution was fed into the syringe pumps (KD Scientific model 100) connected to the metallic needle with the feed rate of 0.1 mL h^{-1}. The metallic needle was attached to a high-voltage power supply (YSTC), and a piece of aluminum foil was placed 6 cm below the tip of the needle to collect the nanofiber. The spinning voltage was set at 10 kV. All experiments were carried out at room temperature.

Measurements

Fourier transform infrared (FT-IR) spectra were recorded on a PerkinElmer Spectrum 100 Model FT-IR spectrometer. Elemental analyses were run in a Heraeus VarioEL-III CHNS elemental analyzer. ^{1}H and ^{13}C NMR spectra were recorded on a Bruker DPX-400 MHz FT-NMR, and peak multiplicity was reported as follows: s, singlet; d, doublet; t, triplet; m, multiplet. The inherent viscosities were determined at 0.5 g dL^{-1} concentration using a Tamson TV-2000 viscometer at 30 °C. Thermogravimetric analysis (TGA) was conducted with a TA Instruments Q50 in flowing nitrogen or air (flow rate = 60 cm^{3} min^{-1}) at a heating rate of 20 °C min^{-1}. Thermal Mechanical Analysis (TMA) was conducted with a TA instrument TMA Q400. The TMA experiments were conducted from 40 to 400 °C at a scan rate of 10 °C min^{-1} with a film/fiber probe under an applied constant load of 5 mN. Ultraviolet-visible (UV-Vis) spectra of the polymer films were recorded on a Hitachi U-4100 spectrometer. Photoluminescence (PL) spectra were recorded with a Fluorolog-3 spectrofluorometer. The relative PL quantum yield (Φ_{PL}) of the samples in different solvents were measured by using quinine sulfate dissolved in 1 N sulfuric acid as a reference standard (Φ_{PL} = 0.546), and the Φ_{PL} of polymer thin films was determined by using a calibrated integrating sphere. All spectra were obtained by averaging five scans. The morphology of the ES fiber was characterized by using an optical microscope (HUVITZ Co., Ltd).

Quantum chemical calculation

The molecular simulation in this study was performed by using the Gaussian 09 program package, which implements analytical gradients at the time-dependent density functional theory (TD-DFT). The DFT method at the Becker style three-parameter density functional theory using the Lee–Yang–Parr correlation functional level of theory (B3LYP) with the 6-31G (d) basis set was adopted for calculating electronic structures and spectroscopic properties of the model compounds.

Results and discussion

Material synthesis

The model compounds of **M-Ph**, **M-Np**, and **M-Py** were synthesized from the corresponding triarylamine-containing dianhydrides (**1–3**) with two equivalents of cyclohexylamine (Scheme 1), and **M-Ph′** was prepared from 4,4′-diamino-triphenylamine (**1′**) and 1,2-cyclohexanedicarboxylic anhydride. Elemental analysis, ^{1}H NMR, ^{13}C NMR, and FT-IR spectroscopic techniques were used to identify the structures of these model compounds as shown in Fig. S1 to S5.† The results of these spectroscopic analyses suggest that the target model compounds were prepared successfully.

The polyimides were synthesized by high-temperature solution polycondensation (Scheme 2). These dianhydrides and bis (4-aminocyclohexyl)methane were polymerized in *m*-cresol at 200 °C in the presence of isoquinoline as a catalyst. The resulting viscous solutions then could be precipitated to obtain

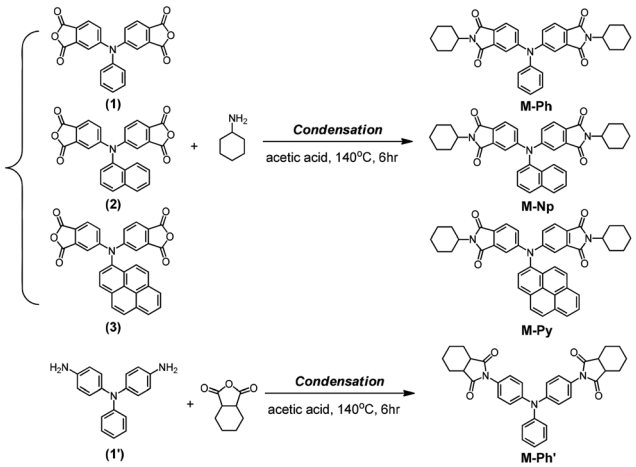

Scheme 1 Synthesis of imide model compounds.

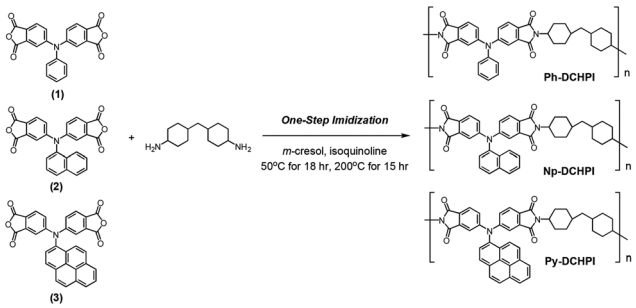

Scheme 2 Synthesis of triarylamine-based polyimides.

tough fiber-like polymers when slowly pouring into methanol. The inherent viscosities and molecular weights of these polymers are summarized in Table S1.† All these high molecular weight polymers could afford transparent and tough films by solution casting as shown in Fig. 1. ^{1}H NMR and FT-IR spectroscopic techniques were used to identify structures of the obtained polyimides, and the results agree well with the proposed molecular structures (Fig. S6 and S7†).

Basic polymer properties

The solubility behavior of these resulting polymers was investigated at 5 mg ml^{-1} concentration, and the results are also

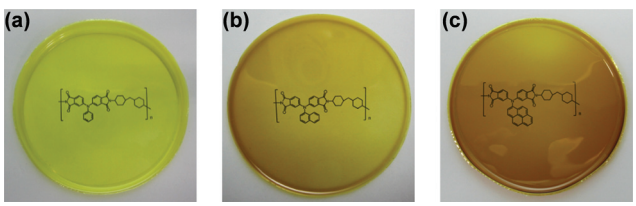

Fig. 1 The photographs of polyimides with thickness around 30 μm. (a) **Ph-DCHPI**, (b) **Np-DCHPI**, and (c) **Py-DCHPI**.

listed in Table S2.† These semi-aromatic PIs were readily soluble in less polar solvents like $CHCl_3$ and THF and high polar aprotic solvents such as NMP and DMAC. Thus, these PIs have potential to be used in spin-coating or inkjet-printing to afford high performance thin films for optoelectronic devices.

Thermal properties of the obtained PIs were examined by TGA and TMA, and the results are summarized in Table S3.† TGA curves of these resulting polymers shown in Fig. S8† exhibited high thermal stability with insignificant weight loss up to 430 °C both under nitrogen and air atmospheres. Typical TMA curves of these resulting PIs are depicted in Fig. S9† and hand glass-transition temperatures (T_g) around 340–386 °C could be obtained, depending upon the stiffness and rigidity of the polymer chain, and the higher T_g of the PI **Py-DCHPI** could be attributed to the rigidity and stronger π–π interactions of pyrene moieties.

Optical properties

Optical behavior of the model compounds was investigated by UV-vis and PL spectroscopy depicted in Fig. 2, and the results are summarized in Table 1. These imide-containing model compounds of **M-Ph**, **M-Np**, and **M-Py** derived from triarylamine-based dianhydrides showed two absorptions at around 222–272 and 378–395 nm, and exhibited PL emission maximum at 433–461 nm in cyclohexane solution (conc.: 10 μM) with PLQY (Φ_{PL}) ranging from 25.7% to 36.0%. While, **M-Ph′** prepared from TPA-based diamine which is a structural isomer of **M-Ph** revealed not only a lower PL quantum yield of 4.3% (Fig. 3) compared with **M-Ph** (Φ_{PL} = 36.0%) but also a

Table 1 Optical properties of the imide model compounds

	Cyclohexane [10 μM] solution, R.T.		
Code	λ_{max}^{abs} [nm]	λ_{max}^{em} [nm] [a]	Φ_{PL} [b] [%]
M-Ph′	311	366	4.3
M-Ph	395	433	36.0
M-Np	388	436	33.4
M-Py	378	461	25.7

[a] They were excited at λ_{max}^{abs} for solution states. [b] The quantum yield was measured by using quinine sulfate (dissolved in 1 N H_2SO_4 with a concentration of 10 μM, assuming photoluminescence quantum efficiency of 0.546) as a standard at 25 °C.

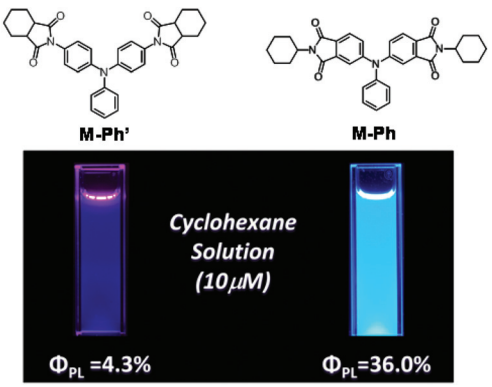

Fig. 3 PL photographs of the model compound solutions **M-Ph** and **M-Ph′** (concentration is 10 μM in cyclohexane) taken under illumination at 365 nm UV light.

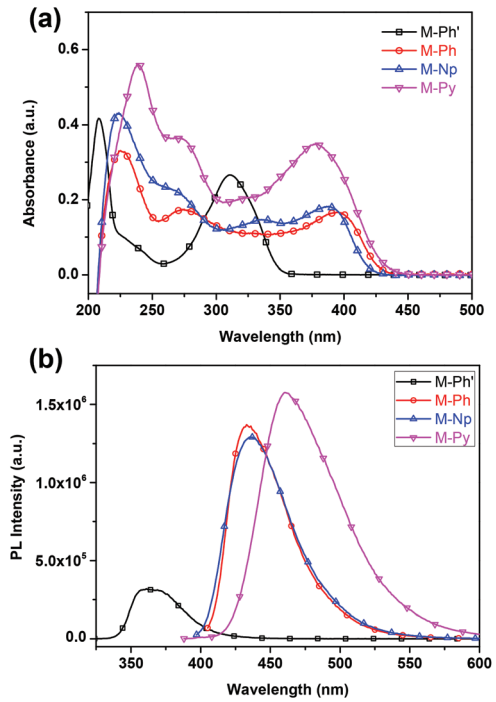

Fig. 2 (a) UV-Vis and (b) PL spectra of model compounds in cyclohexane solution (10 μM).

hypsochromic shift both in the absorptions at 208 and 311 nm, and a PL emission peak at 366 nm. The imide-containing model compounds of **M-Ph**, **M-Np**, and **M-Py** with more extended conjugation phthalimide structures have a lower energy band gap and result in a bathochromic shift of absorption and emission in the UV-Vis and PL spectra, respectively. In order to gain more insight into the photophysical behavior of the conjugated triarylamine-containing phthalimide system, TD-DFT calculations could be used to clarify the nature of electron transitions of the model compounds with different triarylamine-based phthalimide moieties. Calculated molecular orbital diagrams of these model compounds are depicted in Fig. 4, and the excitation wavelengths, the oscillator strengths (f), the contribution molecular orbitals (MOs), the assignments of electron transitions from ground state (S_0) to excited states (S_i), and the contributions of each transition of model compounds are summarized in Table S4.† In the case of **M-Ph**, **M-Np**, and **M-Py**, the MOs related to the lowest excited transition from HOMO to LUMO delocalized over the triarylamine-based phthalimide moieties derived from triarylamine-based dianhydrides, implying that the S_0 to S_1 could be attributed to LE (π–π*) transition. In addition, higher excited transition states such as LUMO+1, LUMO+2, and LUMO+3 of

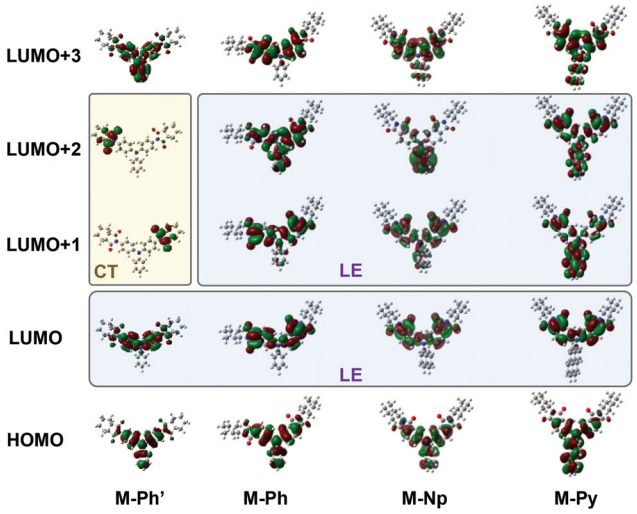

Fig. 4 Calculated molecular orbitals of the model compounds (TD-DFT method at B3LYP/6-31G(d)).

M-Ph, **M-Np**, and **M-Py** also revealed similar LE (π–π*) orbital transitions around the triarylamine-based phthalimide moieties. In the case of **M-Ph′**, the lowest excited transition from HOMO to LUMO also exhibited LE (π–π*) transition, but revealed CT (π–π*) transition from the HOMO of electron-donating diamine units to higher excited LUMO+1 and LUMO+2 states of the electron-accepting anhydride moieties. Therefore, the model compound **M-Ph** derived from TPA-based dianhydride showed higher PL intensity than the isomeric compound **M-Ph′** prepared from the TPA-based diamine.

In addition, all the model compounds of **M-Ph**, **M-Np**, and **M-Py** exhibited solvatochromic PL behavior in different polarity solvents (conc.: 10 μM) as shown in Fig. S12–S14,† and the results are summarized in Tables S5–S7,† respectively. The solvatochromism could be attributed to the fast conversion process from the emissive local excited state to the low emissive state. These results clearly indicate that solvent polarity exerts little effect on absorption behavior, while the PL emission behavior shows strong solvent polarity dependence, resulting in a broad emission band and remarkable bathochromic shift with increasing solvent polarity.

UV-vis absorption and PL emission behavior of the resulting PIs were investigated and depicted in Fig. 5, and PL photographs of these PIs in solution, film, and fiber states were taken under illumination at 365 nm as shown in Fig. 6. These PIs exhibited maximum UV-vis absorption bands at around 378–407 nm in NMP solution (conc.: 10 μM) due to the LE (π–π*) transitions of the triarylamine-based phthalimide luminogens, and revealed yellowish-green PL emission with

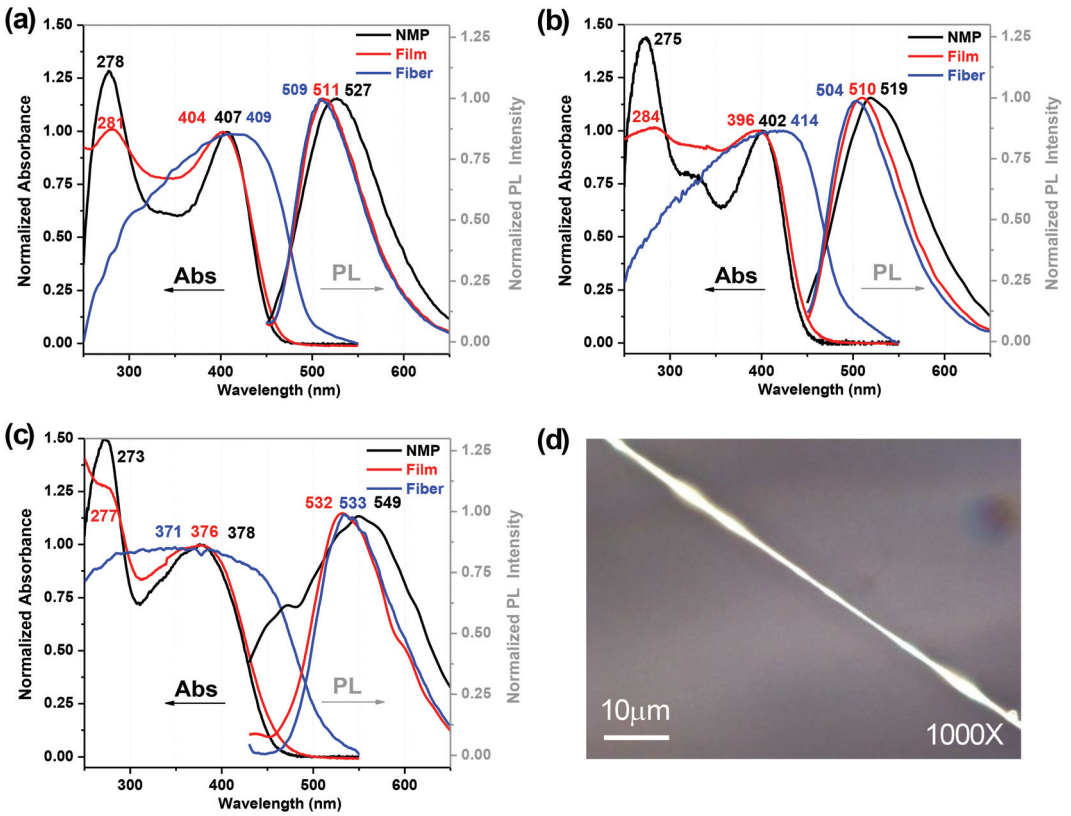

Fig. 5 Absorption and photoluminescence (PL) spectra of the polyimide (a) **Ph-**, (b) **Np-**, and (c) **Py-DCHPI** in solution, film and fiber states. (d) OM image of the **Ph-DCHPI** nanofiber.

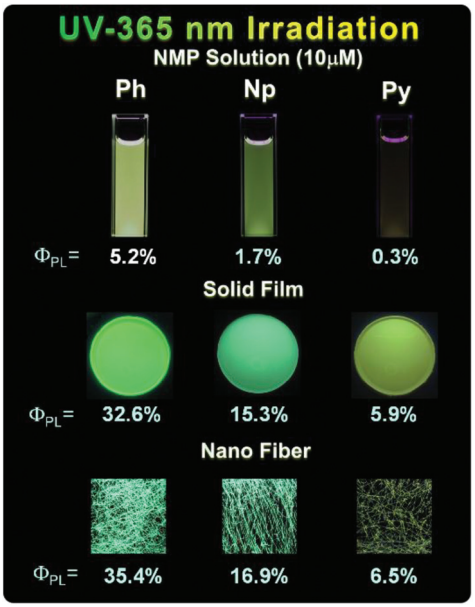

Fig. 6 Photographs of polyimides in solution, film, and fiber states were taken under illumination of a 365 nm UV light.

maximum peaks around 519–549 nm and Φ_{PL} ranging from 0.3 to 5.2%. Interestingly, the resulted PIs revealed much higher Φ_{PL} in the solid film than in the NMP solution with hypsochromic-shifted PL behavior as shown in Fig. 6, and Φ_{PL} of the **Ph-DCHPI** film could be greatly enhanced to 32.6%. Furthermore, the ES fibers were also fabricated to confirm the AEE phenomenon of high Φ_{PL} in the solid state as shown in Fig. 5d and 6. The highly orientated ES fiber of **Ph-DCHPI** exhibited not only a stronger PL intensity with enhanced Φ_{PL} up to 35.4% but also great bathochromic-shift onset absorption when compared with the corresponding solid film (as summarized in Table 2). These luminogenic polymers with AIE and AEE characteristics could be attributed to the triarylamine-based phthalimide moieties. However, the Φ_{PL} increased only slightly from the solution to the film state for **Py-DCHPI** that maybe ascribed to the competition of ACQ (pyrene group) and AIE (triarylamine moiety) effects.

To demonstrate the competition of ACQ and AIE effects on PL behavior, the PI NMP solutions with different methanol fractions were used to investigate the aggregation effect on PL intensity as depicted in Fig. 7, and the results are summarized in Table S8.† By introducing a poor solvent of methanol into the PI NMP solutions, the existing forms of luminogenic moieties could be tuned from solution to aggregated particles in the mixture, resulting in changes in their PL behavior. For instance, **Np-DCHPI** in pure NMP exhibited weak yellowish-green PL emission with a maximum peak at 523 nm, while the emission was slightly blue-shifted and the intensity enhanced simultaneously on increasing the methanol fraction to 30 vol %. The enhancement of PL intensity could be attributed to the AIE effect by the formation of molecular aggregation, and the restriction of luminogen intramolecular rotations results in higher PL intensity. However, by further increasing the methanol fraction more than 50 vol%, the intermolecular π–π stacking enhanced with increasing the extent of aggregation that induced intermolecular energy transfer to decrease the PL intensity and also red-shift in the meantime.

Conclusions

Three high PL efficiency polyimides could be readily prepared *via* one-step polycondensation from triarylamine-based tetracarboxylic dianhydrides and aliphatic diamine, which can suppress the formation of the CT complex. The resulting **Ph-DCHPI** exhibited high PLQY values of 32.6% and 35.4% in the solid film and nanofiber states, respectively. **Py-DCHPI** containing the pyrene group could induce more ACQ than the AIE effect, and reveal a lower PLQY of 5.9% in the film state. In addition, a series of model compounds corresponding to the repeat unit of the PIs were also synthesized, and density functional theory calculations were used to support the deduction. We demonstrate that the model compound **M-Ph′** with central triarylamine diamine showed higher capability to form a charge transfer complex due to CT (π–π*) states, resulting in lower PL intensity, while, the other model compounds derived from triarylamine-based dianhydrides exhibited high LE (π–π*) emission and stronger PL intensity. Moreover, the competition of AIE and ACQ effects of these triarylamine-based PIs was investigated and demonstrated. This comparative study of the isomeric triarylamine-based phthalimide structure effect on

Table 2 Optical properties of the polyimides

	NMP [10 μM] solution, R.T.			Film, R.T.				Nanofiber, R.T.			
Polymer	λ_{max}^{abs} [nm]	λ_{max}^{em} [a] [nm]	Φ_{PL} [b] [%]	λ_{max}^{abs} [nm]	λ_{onset}^{abs} [nm]	λ_{max}^{em} [a] [nm]	Φ_{PL} [c] [%]	λ_{max}^{abs} [nm]	λ_{onset}^{abs} [nm]	λ_{max}^{em} [a] [nm]	Φ_{PL} [c] [%]
Ph-DCHPI	407	527	5.2	404	458	511	32.6	409	497	509	35.4
Np-DCHPI	402	519	1.7	396	453	510	15.3	414	484	504	16.9
Py-DCHPI	378	549	0.3	376	462	533	5.9	371	504	533	6.5

[a] They were excited at λ_{max}^{abs}. [b] The quantum yield was measured by using quinine sulfate (dissolved in 1 N H_2SO_4 with a concentration of 10 μM, assuming photoluminescence quantum efficiency of 0.546) as a standard at 25 °C. [c] PL quantum yields of polymer thin films were determined using a calibrated integrating sphere.

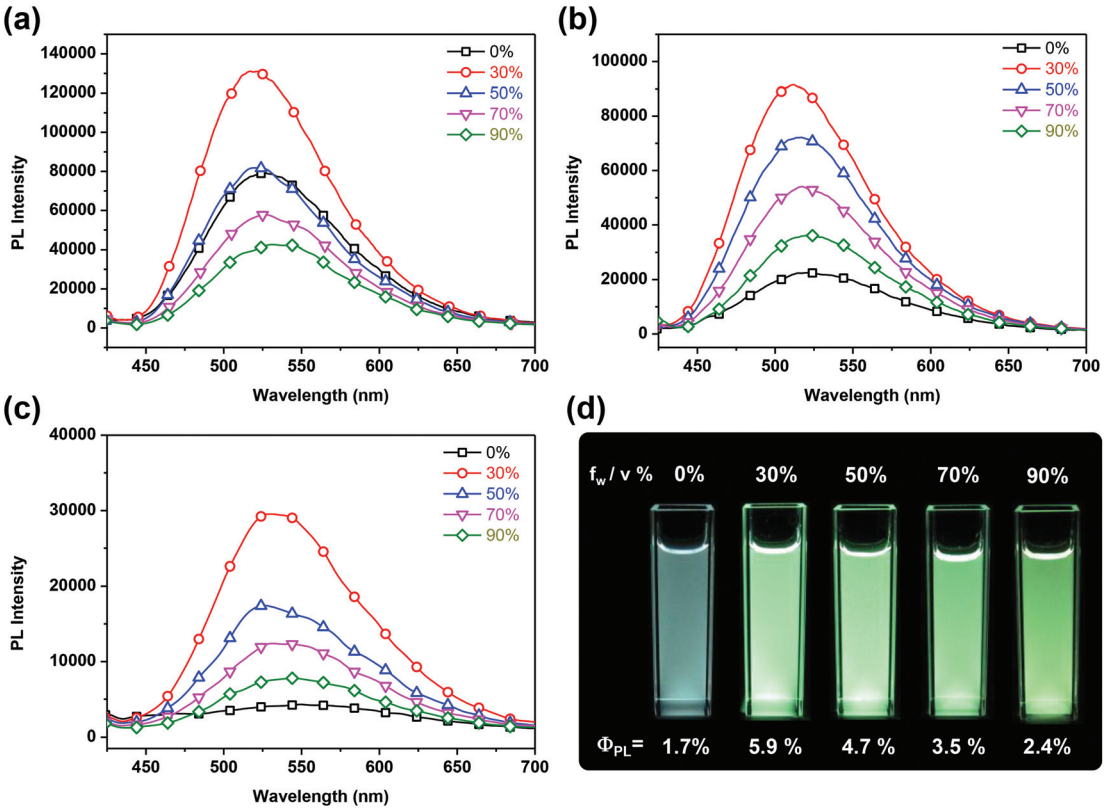

Fig. 7 PL spectra of the polyimides (a) **Ph-**, (b) **Np-**, and (c) **Py-DCHPI** in NMP–MeOH with different methanol fractions (fw/vol%) (concentration is 10 μM). (d) Photographs of **Np-DCHPI** were taken under illumination at 365 nm UV light.

high LE transition and AIE-active behavior may provide some guidance for designing new high-efficiency PL polyimides.

Acknowledgements

The authors are grateful to the Ministry of Science and Technology of Taiwan for the financial support.

Notes and references

1 B. J. de Gans, P. C. Duineveld and U. S. Schubert, *Adv. Mater.*, 2004, **16**, 203.

2 (*a*) R. H. Friend, R. W. Gymer, A. B. Holmes, J. H. Burroughes, R. N. Marks, C. Taliani, D. D. C. Bradley, D. A. Dos Santos, J. L. Bredas, M. Logdlund and W. R. Salaneck, *Nature*, 1999, **397**, 121; (*b*) X. Yang, X. Xu and G. Zhou, *J. Mater. Chem. C*, 2014, **3**, 913; (*c*) M. C. Gather, A. Kohnen and K. Meerholz, *Adv. Mater.*, 2011, **23**, 233.

3 (*a*) R. Xia, G. Heliotis, M. Campoy-Quiles, P. N. Stavrinou, D. D. C. Bradley, D. Vak and D. Y. Kim, *J. Appl. Phys.*, 2005, 98; (*b*) M. D. McGehee and A. J. Heeger, *Adv. Mater.*, 2000, **12**, 1655; (*c*) I. D. Samuel and G. A. Turnbull, *Chem. Rev.*, 2007, **107**, 1272; (*d*) C. Kallinger, M. Hilmer, A. Haugeneder, M. Perner, W. Spirkl, U. Lemmer, J. Feldmann, U. Scherf, K. Müllen, A. Gombert and V. Wittwer, *Adv. Mater.*, 1998, **10**, 920.

4 (*a*) H. N. Kim, W. X. Ren, J. S. Kim and J. Yoon, *Chem. Soc. Rev.*, 2012, **41**, 3210; (*b*) H. N. Kim, Z. Guo, W. Zhu, J. Yoon and H. Tian, *Chem. Soc. Rev.*, 2011, **40**, 79; (*c*) S. W. Thomas III, G. D. Joly and T. M. Swager, *Chem. Rev.*, 2007, **107**, 1339.

5 (*a*) H. Yu and B. Li, *Sci. Rep.*, 2013, **3**, 1674; (*b*) D. J. Sirbuly, M. Law, P. Pauzauskie, H. Yan, A. V. Maslov, K. Knutsen, C. Z. Ning, R. J. Saykally and P. Yang, *Proc. Natl. Acad. Sci. U. S. A.*, 2005, **102**, 7800; (*c*) X. Xing, H. Zhu, Y. Wang and B. Li, *Nano Lett.*, 2008, **8**, 2839; (*d*) L. Persano, A. Camposeo and D. Pisignano, *Prog. Polym. Sci.*, 2015, **43**, 48.

6 (*a*) D. Vak, J. Jo, J. Ghim, C. Chun, B. Lim, A. J. Heeger and D.-Y. Kim, *Macromolecules*, 2006, **39**, 6433; (*b*) J. Liu, J. Zou, W. Yang, H. Wu, C. Li, B. Zhang, J. Peng and Y. Cao, *Chem. Mater.*, 2008, **20**, 4499.

7 G. S. Liou and H. J. Yen, in *Polymer Science: A Comprehensive Reference*, Editon edn, 2012, vol. 5, pp. 497.

8 (*a*) J. Wakita, H. Sekino, K. Sakai, Y. Urano and S. Ando, *J. Phys. Chem. B*, 2009, **113**, 15212; (*b*) J. Wakita, S. Inoue, N. Kawanishi and S. Ando, *Macromolecules*, 2010, **43**, 3594; (*c*) K. Takizawa, J. Wakita, K. Sekiguchi and S. Ando, *Macromolecules*, 2012, **45**, 4764; (*d*) K. Kanosue, T. Shimosaka,

J. Wakita and S. Ando, *Macromolecules*, 2015, **48**, 1777; (*e*) M. Hasegawa and K. Horie, *Prog. Polym. Sci.*, 2001, **26**, 259; (*f*) J. Ishii, S. Horii, N. Sensui, M. Hasegawa, L. Vladimirov, M. Kochi and R. Yokota, *High Perform. Polym.*, 2009, **21**, 282.

9 (*a*) S. A. Lee, T. Yamashita and K. Horie, *J. Polym. Sci., Part B: Polym. Phys.*, 1998, **36**, 1433; (*b*) Q. Li, K. Horie and R. Yokota, *J. Photopolym. Sci. Technol.*, 1997, **10**, 49.

10 (*a*) A. Qin, J. W. Y. Lam and B. Z. Tang, *Prog. Polym. Sci.*, 2012, **37**, 182; (*b*) Y. Hong, J. W. Y. Lam and B. Z. Tang, *Chem. Soc. Rev.*, 2011, **40**, 5361.

11 (*a*) A. Iwan and D. Sek, *Prog. Polym. Sci.*, 2011, **36**, 1277; (*b*) H. J. Yen, C. J. Chen and G. S. Liou, *Adv. Funct. Mater.*, 2013, **23**, 5307; (*c*) J. H. Wu and G. S. Liou, *Adv. Funct. Mater.*, 2014, **24**, 6422.

12 (*a*) H. J. Yen, C. J. Chen and G. S. Liou, *Chem. Commun.*, 2013, **49**, 630; (*b*) H. J. Yen and G. S. Liou, *Chem. Commun.*, 2013, **49**, 9797; (*c*) H. J. Yen, J. H. Wu, W. C. Wang and G. S. Liou, *Adv. Opt. Mater.*, 2013, **1**, 668.

13 (*a*) W. Z. Yuan, P. Lu, S. Chen, J. W. Y. Lam, Z. Wang, Y. Liu, H. S. Kwok, Y. Ma and B. Z. Tang, *Adv. Mater.*, 2010, **22**, 2159; (*b*) Y. Zhang, G. Chen, Y. Lin, L. Zhao, W. Z. Yuan, P. Lu, C. K. W. Jim, Y. Zhang and B. Z. Tang, *Polym. Chem.*, 2015, **6**, 97; (*c*) J. Qian, Z. Zhu, A. Qin, W. Qin, L. Chu, F. Cai, H. Zhang, Q. Wu, R. Hu, B. Z. Tang and S. He, *Adv. Mater.*, 2015, **27**, 2332; (*d*) L. Li, M. Chen, H. Zhang, H. Nie, J. Z. Sun, A. Qin and B. Z. Tang, *Chem. Commun.*, 2015, **51**, 4830; (*e*) Y. Lin, G. Chen, L. Zhao, W. Z. Yuan, Y. Zhang and B. Z. Tang, *J. Mater. Chem. C*, 2015, **3**, 112; (*f*) J. Li, Y. Jiang, J. Cheng, Y. Zhang, H. Su, J. W. Y. Lam, H. H. Y. Sung, K. S. Wong, H. S. Kwok and B. Z. Tang, *Phys. Chem. Chem. Phys.*, 2015, **17**, 1134; (*g*) C. Y. K. Chan, J. W. Y. Lam, C. Deng, X. Chen, K. S. Wong and B. Z. Tang, *Macromolecules*, 2015, **48**, 1038.

